Supporting Information

Metallo-boranes: A Class of unconventional superhalogens defying electron counting rules

Huta Banjade, Hong Fang, and Puru Jena

Physics Department, Virginia Commonwealth University, Richmond, VA 23284

Table S1. Point group symmetries of the studied clusters and their HOMO-LUMO gap (Δ_G) in the anionic state.

Cluster	Symmetry	Δ_G (eV)
$Zn(B_{12}H_{12})$	C_s	5.91
$Al(BeB_{11}H_{12})$	C_s	5.05
$ZnB_{12}H_{11}$	C_s	4.46
$AlB_{12}H_{12}$	C_s	7.56
$Zn(CB_{11}H_{12})$	C_1	5.52
$Zn(BeB_{11}H_{12})$	C_1	5.47
$LiB_{12}H_{12}$	C_1	6.03

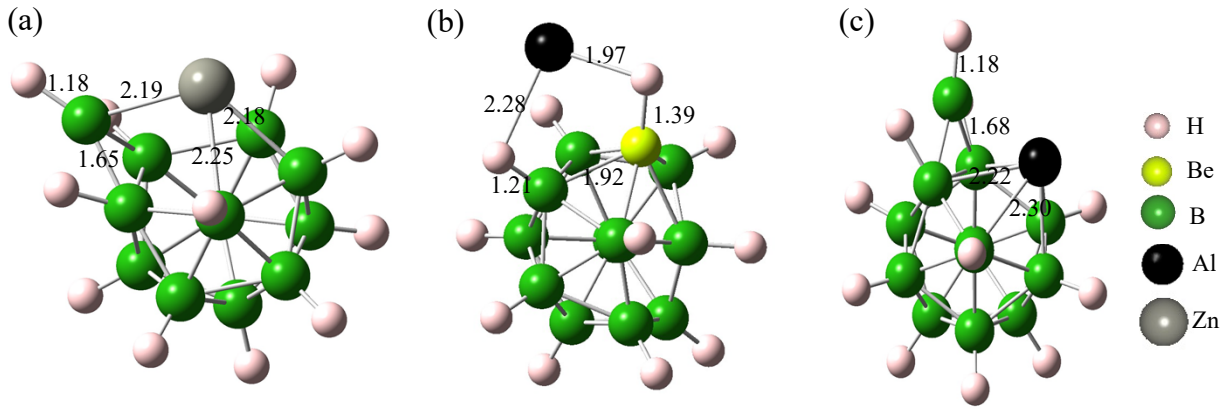

Figure S1. Higher energy isomer of the (a) $Zn(B_{12}H_{12})$, (b) $Al(BeB_{11}H_{12})$, and (c) $Al(B_{12}H_{12})$ clusters. Isomer for $Al(B_{12}H_{12})$ is 2.04 eV higher in energy than the one presented in Figure 4(b). The characteristic bond length (in Å) between different atoms is shown in the Figure.

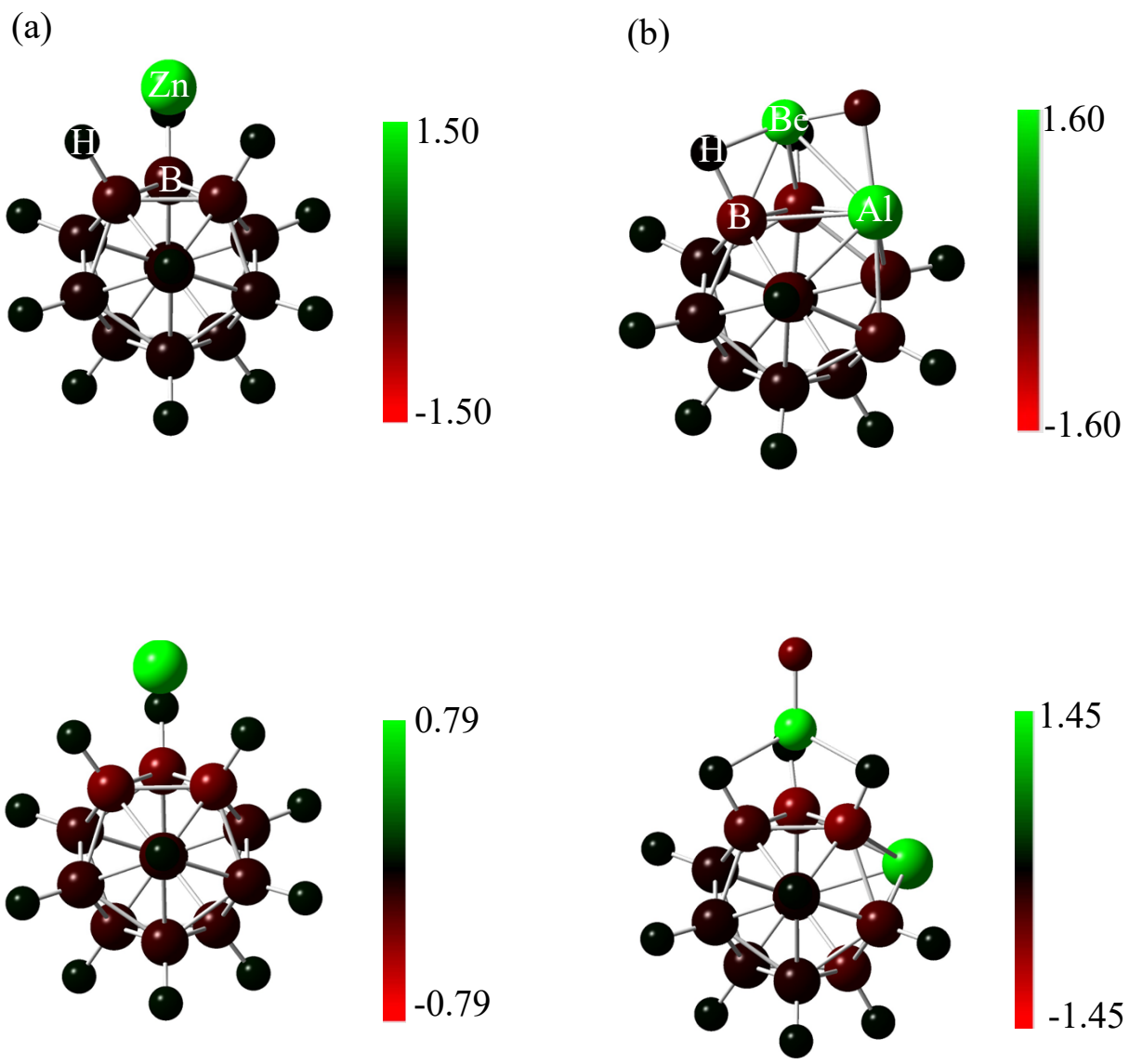

Figure S2. Natural charge distribution; neutral (top panel) and anion (bottom panel) in (a) $Zn(B_{12}H_{12})$, and (b) $Al(BeB_{11}H_{12})$.

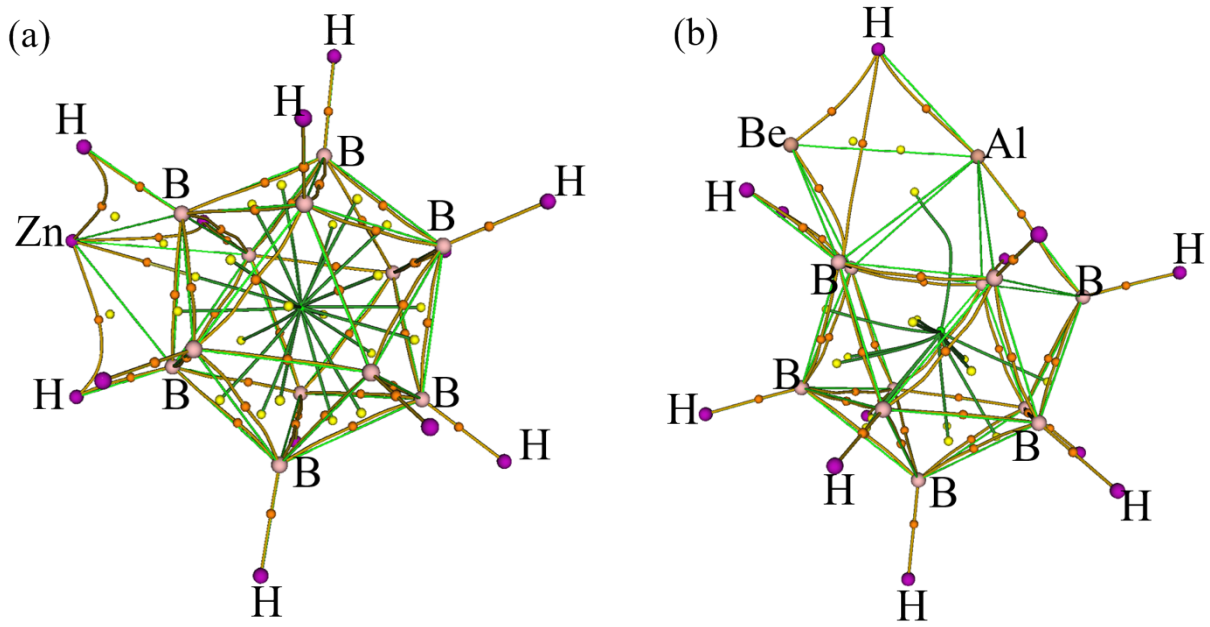

Figure S3. Molecular graph showing the bond critical points (orange dots), ring critical points (yellow), cage critical points (green), and the bond paths in (a) $Zn(B_{12}H_{12})$ and (b) $Al(BeB_{11}H_{12})$. Solid brown is the bond path connecting the two-atom critical point, and light green represents the bond connecting two atoms. In contrast, the dark green lines are the paths connecting the cage and ring critical points.

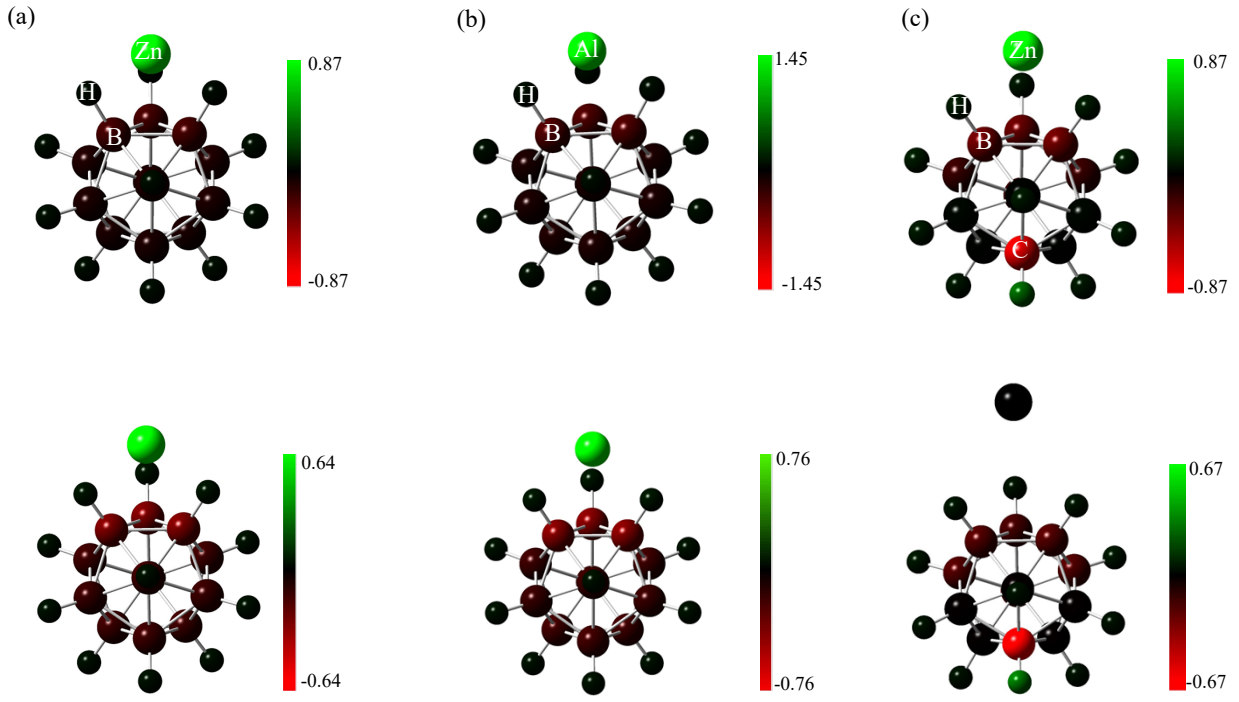

Figure S4. Natural charge distribution; neutral (top panel) and anion (bottom panel) in (a) $Zn(B_{12}H_{11})$, (b) $Al(B_{12}H_{12})$, and (c) $Zn(CB_{11}H_{12})$.

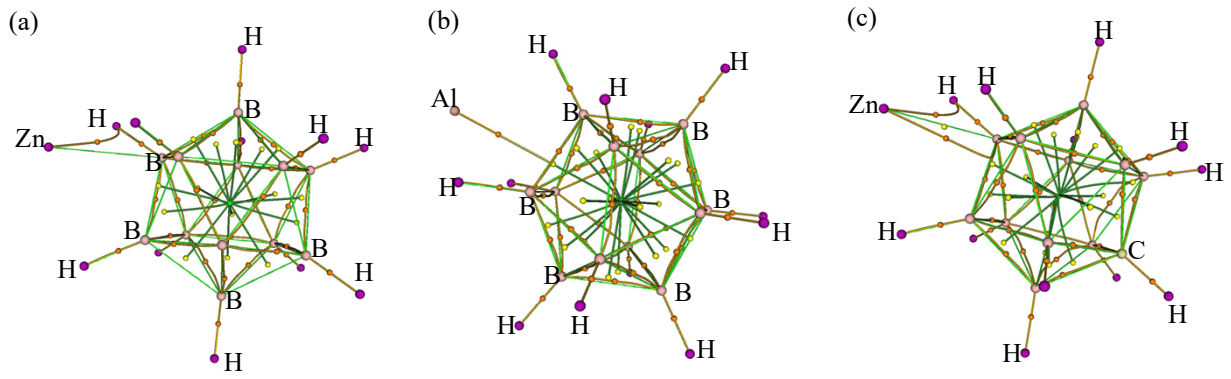

Figure S5. Molecular graph showing the bond critical points (orange dots), ring critical points (yellow), cage critical points (green), and the bond paths in (a) $Zn(B_{12}H_{11})$, (b) $Al(B_{12}H_{12})$, and (c) $Zn(CB_{11}H_{12})$. Solid brown is the bond path connecting the two-atom critical points, and light green represents the bond connecting two atoms. In contrast, dark green is the path connecting the cage and ring critical points.

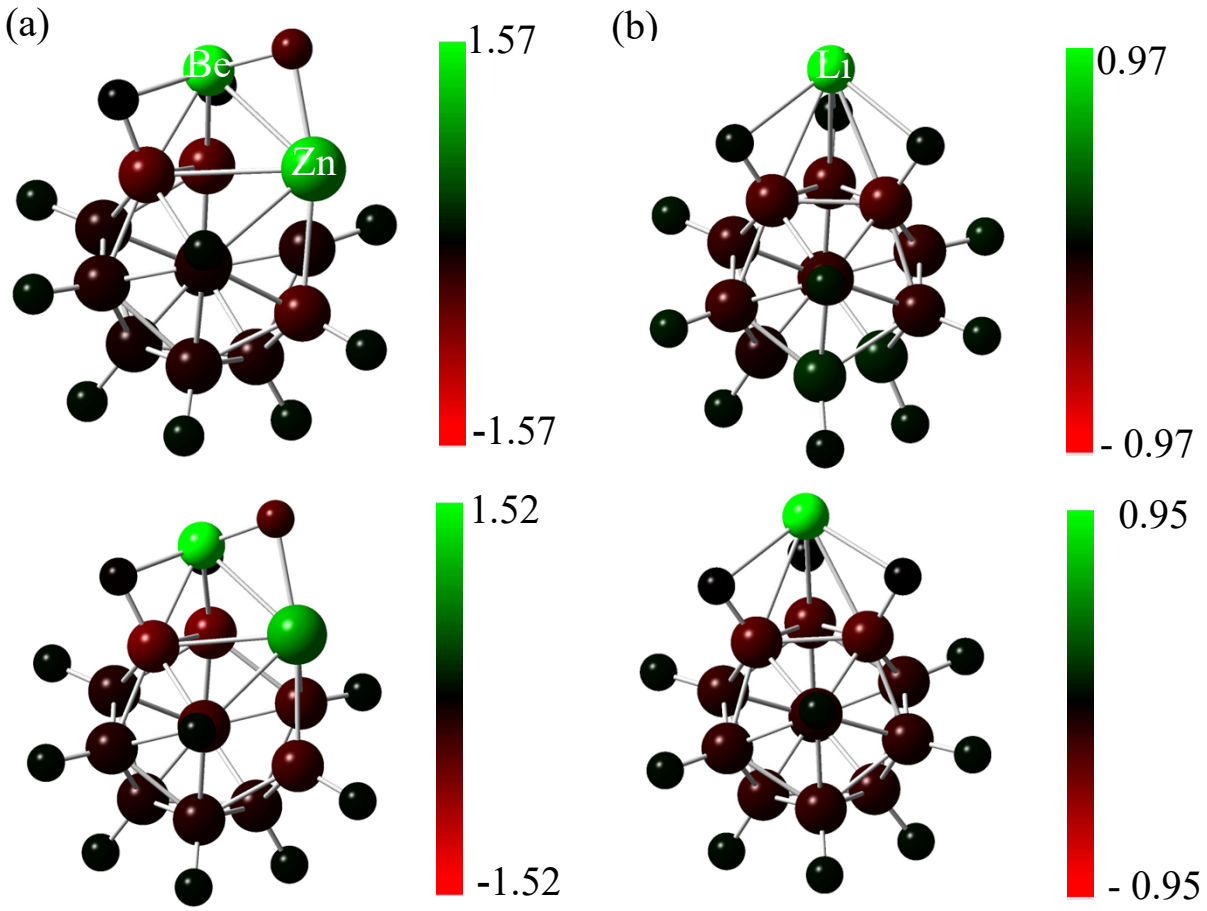

Figure S6. Natural charge distribution; neutral (top panel), and anion (bottom panel) in (a) $Zn(BeB_{11}H_{12})$and (b) $Li(B_{12}H_{12})$.

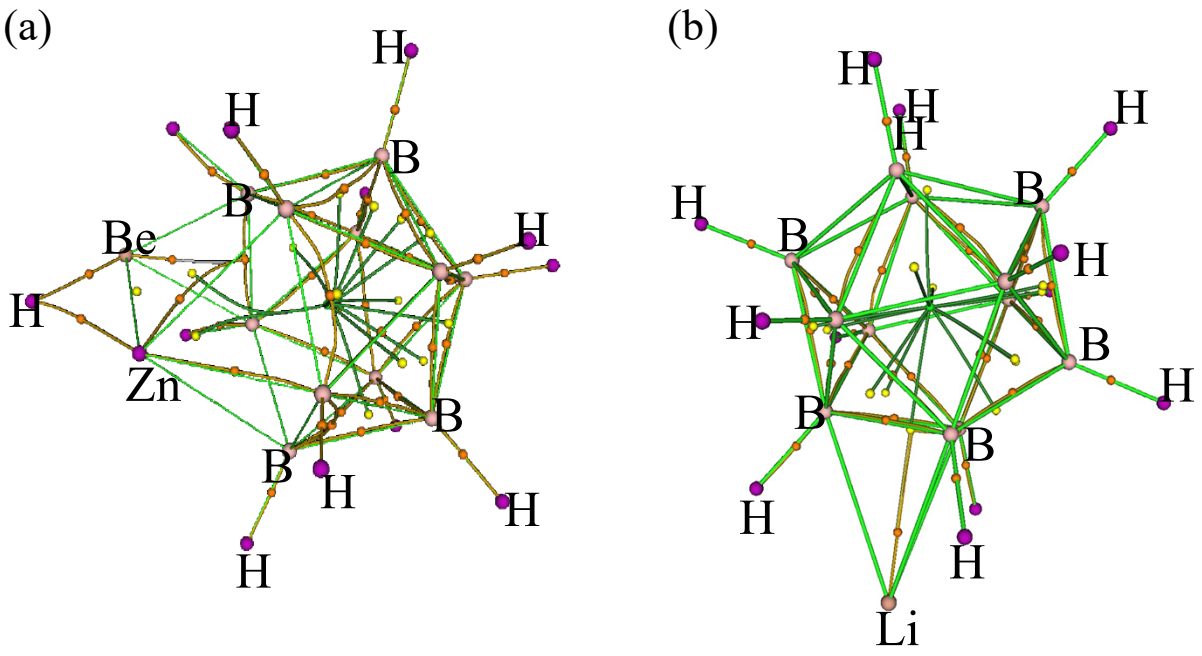

Figure S7. Molecular graph showing the bond critical points (orange dots), ring critical points (yellow), cage critical points (green), and the bond paths in (a) $Zn(BeB_{11}H_{12})$, and (b) $Li(B_{12}H_{12})$. Solid brown is the bond path connecting the two-atom critical point, and light green represents the bond connecting two atoms. At the same time, the dark green is the path connecting the cage and ring critical points.

Kinetic stability test of the clusters

To test the atomic vibrational stability under thermal excitation of the clusters we performed ab initio molecular dynamics (AIMD) simulation of $Zn(B_{12}H_{12})$ and $Al(B_{12}H_{12})$ clusters by using density functional theory calculations as implemented in the Vienna *ab initio* simulation package (VASP).[1] Generalized gradient approximation and the Perdew-Burke-Ernzerhof (PBE)[2] exchange-correlation functional are used to describe the electron exchange-correlation. To avoid the interaction between the periodic images, we used a vacuum padding of 15 Å in each

direction during AIMD. The system is confined to an NVT ensemble at 300 K for 5 ps. The configurations after AIMD simulations shown in Figure S8 show the thermal stability at 300 K.

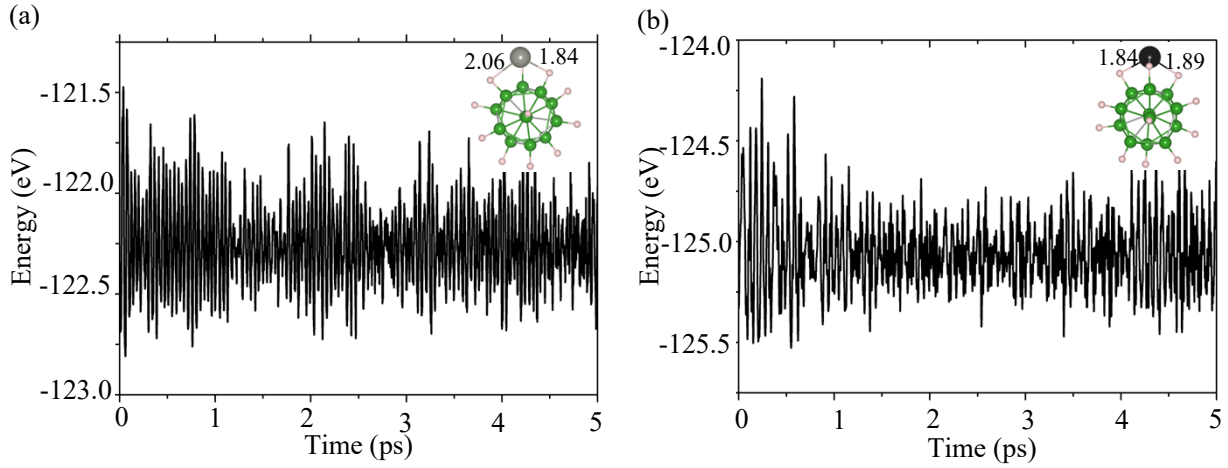

Figure S8: Energy evolutions of the $Zn(B_{12}H_{12})$ and $Al(B_{12}H_{12})$ cluster during 5 ps AIMD simulation at 300 K.

Supplementary Reference:

1 G. Kresse and J. Furthmüller, Efficiency of ab-initio total energy calculations for metals and semiconductors using a plane-wave basis set, *Comput. Mater. Sci.*, 1996, **6**, 15–50.

2 J. P. Perdew, K. Burke and M. Ernzerhof, Generalized Gradient Approximation Made Simple, *Phys. Rev. Lett.*, 1996, **77**, 3865–3868.